ARTICLE

Designing the Electric Transport Characteristics of ZnO Micro/Nanowire Devices by Coupling Piezoelectric and Photoexcitation Effects

Youfan Hu, Yanling Chang, Peng Fei, Robert L. Snyder, and Zhong Lin Wang*

School of Material Science and Engineering, Georgia Institute of Technology, Atlanta, Georgia 30332-0245

ABSTRACT The localized coupling between piezoelectric and photoexcitation effects of a ZnO micro/nanowire device has been studied for the first time with the goal of designing and controlling the electrical transport characteristics of the device. The piezoelectric effect tends to raise the height of the local Schottky barrier (SB) at the metal−ZnO contact, while photoexcitation using a light that has energy higher than the band gap of ZnO lowers the SB height. By tuning the relative contributions of the effects from piezoelectricity *via* strain and photoexcitation *via* light intensity, the local contact can be tuned step-by-step and/or transformed from Schottky to Ohmic or from Ohmic to Schottky. This study describes a new principle for controlling the coupling among mechanical, photonic, and electrical properties of ZnO nanowires, which could be potentially useful for fabricating piezo-phototronic devices.

KEYWORDS: ZnO · nanowire · Schottky contact · piezoelectricity · photoexcitation · piezo-phototronics

Semiconductor nanowires are the fundamental materials for fabricating a wide range of nanodevices.[1−5] In the oxide family, ZnO nanowires and nanobelts have been widely studied as a key 1D oxide nanomaterial for numerous applications. Due to the unique piezoelectric and semiconducting coupled properties, a range of novel nanodevices of ZnO have been developed, such as nanogenerators,[6−9] piezoelectric field effect transistors,[10] piezoelectric diode,[11] and strain sensors.[12] A direct band gap of 3.4 eV and a large exciton binding energy (60 meV) at room temperature make ZnO a prominent candidate in optical applications, such as an ultraviolet detector,[13−16] optical pumped laser,[17,18] and light emitting diodes.[19] Recently, the photoconducting response at different degrees of straining of a ZnO nanowire has been studied using *in situ* transmission electron microscopy.[20] Although a lot of progress has been made in each research field as stated above, very limited research has been conducted on the localized and quantitatively controlled coupling of the piezoelectric effect and photoexcitation on a ZnO nanowire nanodevice.

In this paper, by introducing a controllable stepping strain and using a focused laser beam, we have investigated the localized coupling between the piezoelectric effect and photoexcitation of ZnO microwire devices that exhibit various controlled electrical transport characteristics. By using microwire devices with Schottky−Ohmic, Ohmic−Ohmic, and Schottky−Schottky contacts, we have demonstrated the fine-tuning of contact characteristics, such as from Schottky to Ohmic or from Ohmic to Schottky, by varying the individual contributions made by piezoelectricity and photoexcitation at local contacts. On the basis of this concept, a design of electric transport properties is demonstrated. This study reveals a new principle for controlling the coupling among mechanical, electrical, and optical properties, which can be the basis for fabricating piezo-photonic-electronic nanodevices, which is referred to as piezo-phototronics.

RESULTS AND DISCUSSION

Our device was fabricated using a single micro/nanowire of ZnO (see the Experimental Methods for details). First, we investigated the photoresponse of a microwire device with photoexcitation at different locations along the ZnO microwire. Figure 1a is a superimposed optical image taken from a ZnO microwire device with the laser spot focused at different positions, as schematically shown on the right-hand side. Points P1, P2, and P3, respectively, represent the positions at the left-hand metal−ZnO contact, central channel region, and right-hand metal−ZnO contact.

*Address correspondence to zlwang@gatech.edu.

Received for review December 10, 2009 and accepted January 05, 2010.

Published online January 15, 2010. 10.1021/nn901805g

Figure 1b shows the $I-V$ curves recorded with the laser spot at the corresponding positions. The inset is a logarithm plot of the current as a function of the applied voltage showing the change in the magnitude of the current. Originally, the $I-V$ characteristic without laser irradiation is symmetrically nonlinear (black curve), which indicates that Schottky barriers (SBs) were formed at the two contacts with similar barrier heights. When the laser was focused at the left-hand or right-hand metal−ZnO contact, there was a much greater photoresponse when the SB was reversely biased than when it was forward biased. The relative change in the photoconductance reached as much as 3 orders of magnitudes for the local SB when it was reversely biased *versus* forward biased, and a very nonsymmetrical $I-V$ characteristic was observed (red and blue curves). However, when the laser was focused at the channel center, for example, the microwire only, far from each metal−ZnO contact, a symmetric $I-V$ characteristic was seen (green curve), and the photoresponse was moderate compared to the reverse biased SB case. The shape of the $I-V$ curve in this case (green curve) is similar to that of the as-fabricated device without laser excitation (black curve) except for the increase in magnitude (see the inset logarithm plot).

The result presented in Figure 1b can be understood from the mechanism of photoexcitation at a SB. When a SB is formed at the metal−ZnO interface, negative charges build up at the metal surface in a very thin layer. An equal amount of positive charge must exist in the ZnO depletion region.[22] Thus a strong local electric field is formed in the depletion region. Under the irradiation of a light source with energy greater than the band gap, electrons in ZnO's valence band will be excited into the conduction band, leaving holes in the valence band. These photon-generated carriers will contribute to the current only when they can drift or diffuse into the electrode before recombination occurs. If the laser irradiation occurs at the depletion region or at a location less than a diffusion length away from it, the photon-generated electrons and holes are quickly swept away from this area in opposite directions by the strong local electric field in the region, as indicated in the left part of Figure 1c. Therefore, the recombination rate in this area will be greatly depressed, and the local conductance is greatly enhanced. Moreover, the migration of holes into the metal side and the generated electrons in the depletion layer will reduce the local net charge density in the region, thus, the local electric field is lowered, resulting in a reduced height of the SB, as shown at the right-hand part of Figure 1c. When the SB is reversely biased, the applied electric field is parallel to the local electric field in the depletion region, resulting in a large enhancement in the photoconductivity. This is also the working principle of photodiodes. In the case of a forward biased SB, two scenarios have to be considered. One,

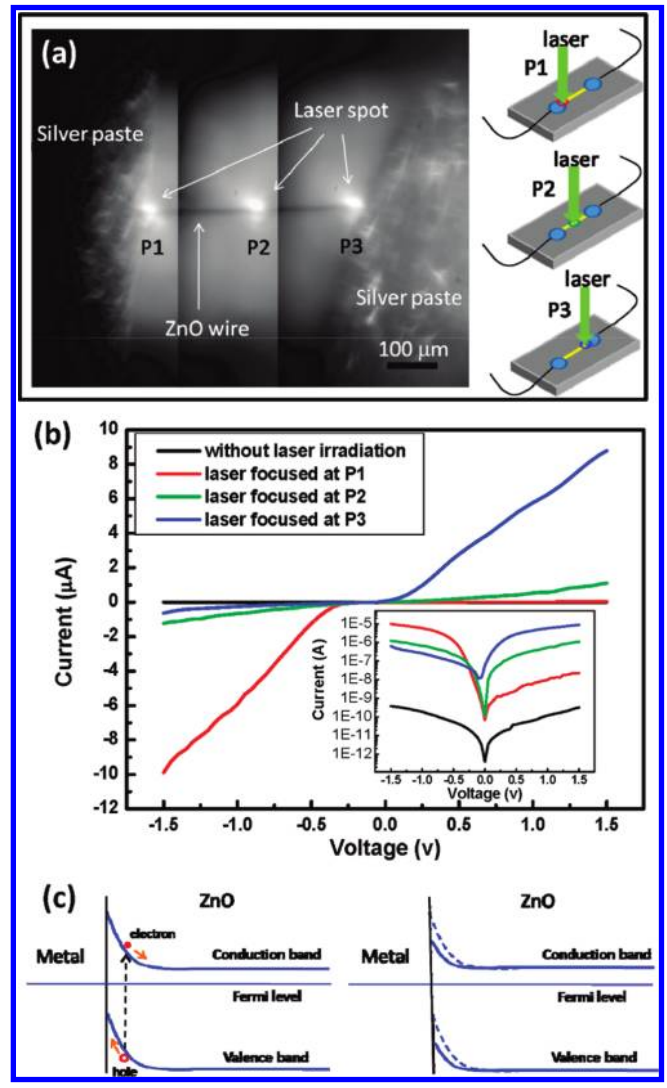

Figure 1. (a) Superimposed optical image taken from a ZnO microwire device with laser spot irradiation at different positions, as indicated. The right-hand side is the corresponding schematic sketches of the relative positions of the laser on the device. (b) $I-V$ curves recorded at corresponding laser focused positions on the device. The inset is a logarithm plot of the absolute value of the current for the $I-V$ curves for illustrating the change in the entire voltage range. (c) Schematic band diagrams of a metal−ZnO SB contact under laser excitation.

when the applied voltage is low, the applied electric field is opposed to the local electric field and not much change in the local conductance is expected. Second, when the applied voltage is high enough, there is no barrier seen by the electrons, and thus no strong local electric field to effectively separate the photon-generated electrons and holes, thus, they have limited contribution to the conductance. Therefore, as a whole, the photoresponse of the forward biased SB has a much smaller effect than in the reverse biased case in tuning the local electric transport property. A sketch of the mechanism stated above is summarized in Figure S1 (Supporting Information).

When the excitation is focused at the central channel of the wire far from the two end contacts, there is

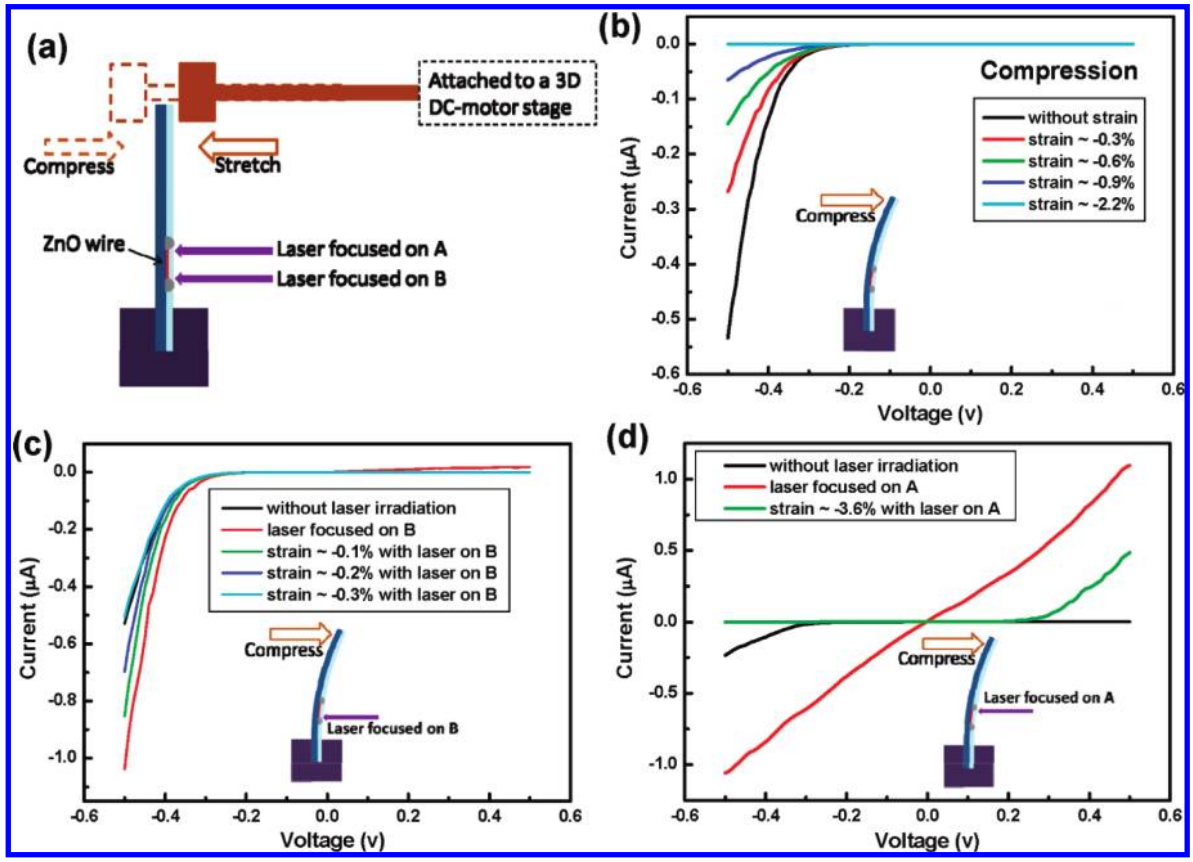

Figure 2. (a) Schematic sketch of the experimental setup for studying the piezoelectricity and photoexcitation coupling effects. (b) *I*−*V* curves of a device, which has Schottky−Ohmic contacts ("diode-like" *I*−*V* curve), when it is compressed to different degrees of strain to illustrate the effect of piezoelectricity on its electric transport characteristic. (c) *I*−*V* curves of the device when both a compressive strain and laser excitation at contact B are introduced, in which the intensity of the laser illumination is kept the same but the degree of straining is varied. (d) Transforming the original diode-like *I*−*V* curve into linear behavior solely by laser irradiation at contact A, and then back to diode-like again with opposite polarity by introducing sufficient strain in the microwire.

only an effect of photon-induced generation of electrons and holes. However, the recombination rate is much higher in this region than in the reverse biased SB area. So the photoresponse is much smaller here compared to the reverse biased SB case. It must be noted that, if the original carrier density is very high, the photon-generated carriers will have limited influence on the conductance. This is the case presented in Figure 3a.

We have also investigated the photoresponse of the device used for Figure 1 when the energy of the light source is less than the band gap (441.6 and 633 nm). Since the defects in the microwires were rather low, as indicated by the corresponding photoluminescence (PL) spectra shown in Figure S2b (Supporting Information), no response was received from the device to the excitation of these two wavelengths regardless of their illuminating position either at the contact or at the microwire (Figure S2a). This result is consistent with the working principle of the devices as stated above.

The next sets of experiments were to investigate the coupling of piezoelectricity and the photoexcitation on the performance of the devices. A controllable strain was introduced in the ZnO microwire devices in conjunction with the laser excitation, as shown schematically in Figure 2a. One end of the device's PS substrate was mounted on a sample holder and tightly fixed. A three-dimensional (3D) DC-motor stage with digital motion controller was used to compress or stretch the free end of the PS substrate. It was assembled with three DC linear stages (MFA-CC, Newport Corp.) in a *x*-*y*-*z* configuration and has a motion resolution of 0.0175 μm according to the manufacturer. The whole set was placed in the light path of a He−Cd laser on an optical table. The position of the device was adjusted to get the laser beam focused at different positions on the device. The related position of the laser spot on the device was monitored using a CCD. As presented in Figure 1, the photoresponse is much larger at the metal−ZnO SB contact than at the microwire, so our study mainly focused on the contacts. For easy notation, we refer to the upper side contact area as A and the lower side one as B, as indicated in Figure 2a. Our study will be presented for devices with three types of *I*−*V* characteristics.

Schottky−"Ohmic" Contacted Device. First, for a device with a diode-like *I*−*V* characteristic, as shown in Figure 2b, the contacts at the two ends are likely to be

very different; one has a higher SB, and the other has a lower or zero height SB, such as Ohmic contact. By considering that the diameter of the microwire was much smaller than the thickness of the PS substrate, and the length of the substrate was much longer than the length of the microwire, the mechanical behavior of the entire system was dominated by the substrate, and a bending of the PS substrate produced solely a tensile or compressive strain in the microwire depending on its bending direction. The strain in the microwire was quantified by the distance at which the substrate was deflected.[12] In Figure 2b, by increasing the strain step-by-step, the diode-like *I*−*V* characteristic finally changed into a totally off status across the entire voltage range. It worked like a piezoelectric switch, showing a huge transformation in the electrical transport characteristic by the piezoelectric effect. As presented in our former systematic studies,[23] when a stress is applied in parallel to the microwire-based device, which is usually parallel to the *c*-axis, a piezoelectric potential gradient is introduced along the microwire due to the polarization of the ions in the crystal. As a result, the electron energy barrier between ZnO and metal electrode will be raised at one side and lowered at the other side if the doping concentration is rather low. In addition, strain will cause band structure to change slightly, which is the piezoresistance effect. The variation introduced by piezoresistance at the two ends of the microwire is identical and will not introduce nonsymmetric *I*−*V* transport behavior. Therefore, if straining introduces an obviously nonsymmetrical change in the *I*−*V* characteristics, the piezoelectric potential is likely the dominant contributor. As for n-type ZnO, although the free carriers in ZnO will partially screen the positive piezoelectric potential, the negative piezoelectric potential is almost unaffected.[24] The increase in SB height at one side with negative piezoelectric potential is likely to be much more pronounced than at the other side that has almost no change in SB height.[23] This is the origin of the piezoelectricity introduced nonsymmetric *I*−*V* transport property in micro/nanowires.

We then introduced laser excitation to the device at the two ends with very different SB heights. First, we introduced the focused laser beam to irradiate at the contact B (Figure 2c), which had a lower SB height. The current increased for the entire voltage, especially the negative voltage range. By fixing the laser spot at this position, and increasing the strain step-by-step, the *I*−*V* curve finally recovered back to its original state when no strain and no laser were applied (Figure 2c). The piezoelectricity and photoexcitation thus have equivalent but opposite effects on the electric transport characteristic of the device. The observed result can be elucidated from

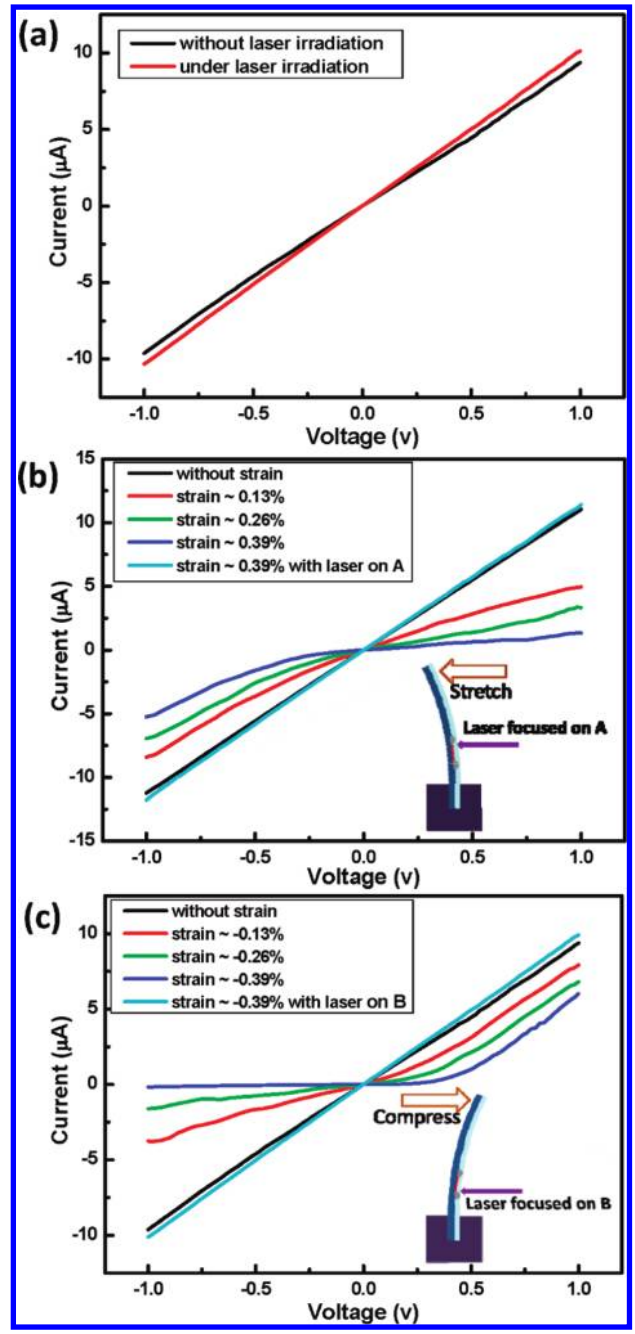

Figure 3. (a) *I*−*V* curves of a device that is dominated by Ohmic contacts, showing its negligible response to the irradiation of laser. (b) Tuning and transforming the *I*−*V* characteristic of the device solely by introducing a tensile strain. An irradiation of the strained device at contact A by the laser recovers its original *I*−*V* characteristic. (c) Tuning and transforming the *I*−*V* characteristic of the device solely by introducing a compressive strain. Note the change in polarity of the "diode-like" transport characteristic. Again, an irradiation of the strained device at contact B by laser recovers its original *I*−*V* characteristic.

the change in SB height. Using the method described in ref 12, we can derive the change in SB height during the compressive deformation, and the result was 19 meV. This value was also the effective decrease in SB height caused by the laser irradiation. In the optical excitation process, the effective SB height change comes from two parts. One is the

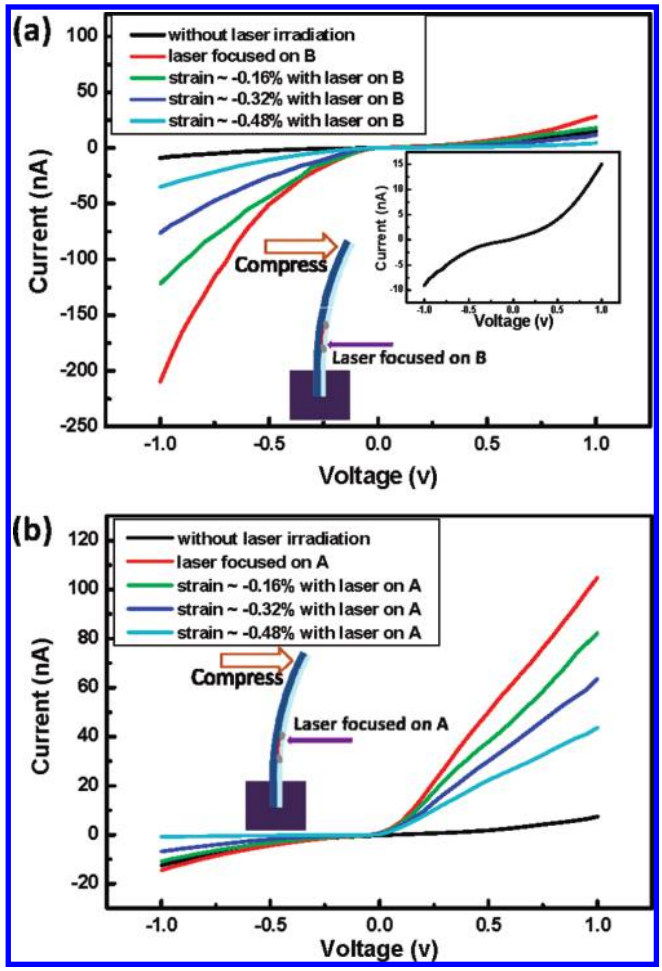

Figure 4. (a) *I*−*V* curves of a device that has Schottky−Schottky contacts when it is compressively stained step-by-step with the laser focused at contact B. The symmetric *I*−*V* curve of the original device is shown in the inset. (b) *I*−*V* curves of the device when it is compressively stained step-by-step with the laser focused at contact A. This figure shows the control in polarity and fine-tuning of its electronic transport characteristic by the coupling of the piezoelectric and photoexcitation properties.

photon-induced carrier density increase, which can be equivalently attributed to a decrease in SB height. The other part is the real SB height decrease due to the weakening of the local electric field in the depletion region under irradiation.

When we moved the focused laser beam to the contact A (Figure 2d), which had a higher SB height, the original diode-like *I*−*V* curve was changed into almost linear and symmetric (red curve). After introducing sufficient compressive strain, the *I*−*V* curve was recovered back to the diode-like characteristic but with opposite rectifying directions (green curve). This experiment shows that the piezoelectric effect and photoexcitation both exist and have opposite effects on the SB height, and using this, we can fully tune the *I*−*V* characteristic of the device.

Ohmic−Ohmic Contacted Device. The second type is an Ohmic−Ohmic contacted device with a linear *I*−*V* curve. In this case, there was no SB or a SB with very small height at each contact. We checked the photoresponse first and found that there was no obvious difference regardless of whether the laser beam was focused at the contact area or at the channel center, and the magnitude of response was negligibly small, as shown in Figure 3a. The conductivity of this ZnO microwire was much higher than the devices with the diode-like *I*−*V* curves, which indicates its higher carrier density. Because there was no obvious SB at the contact, which means that no strong local electric field existed at the interface, the photoelectric response should show no difference regardless of the irradiation position of the laser. A tiny increase in conductance was observed from the photon-induced increase in carrier density in the microwire. As we stated before, when the original carrier density was high, the newly generated carriers only added a small contribution to the final conductivity. In addition, the existence of high density free n-type carriers in the microwire makes the screen effect more effective at the side with a positive piezoelectric potential created by mechanical straining, but the negative piezoelectric potential preserves it.[24] Keeping this in mind, we could introduce a major increase in the SB height on either side of the device by switching the polarity of the piezoelectric potential by changing the sign of the strain through stretching or compressing of the ZnO microwire. The corresponding experimental results are shown in Figure 3b,c. When the focused laser beam was introduced to irradiate the contact with a SB created by the piezoelectric potential, the diode-like *I*−*V* curves were turned back into linear in both cases. One of the most important things that must mentioned here is that, compared to the tiny photoconductance response of the original device with a linear *I*−*V* characteristic, the tuning in current by the laser after a SB being introduced in the device can be as high as 3 orders of magnitude, indicating that the SB can play a very important role for improving the photon sensitivity and spatial resolution in sensor applications.[16,25]

Schottky−Schottky Contacted Device. Finally, we investigated a device that has almost equal SB height at both ends, with a nearly symmetrical nonlinear *I*−*V* characteristic as represented by the dark curve in the inset of Figure 4a. By irradiating at contact A with a focused laser beam, the symmetrical *I*−*V* characteristic was changed into a highly nonsymmetrical one. This means that the SB height at the irradiated end was largely suppressed by the laser beam. Then, fixing the laser spot at contact A and introducing a compressive strain, the *I*−*V* characteristic was tuned step-by-step with a great reduction in current and finally became a diode-like one (see Figure 4a). By shifting the laser spot to contact B, the nonsymmetric polarity of the *I*−*V* transport characteristic was switched (Figure 4b). Again, applying a compressive

strain resulted in a similar effect as for contact A. The data clearly show the effect of the coupling of piezoelectricity and photoexcitation in transforming a device that has Schotty−Schottky contacts into Schotty−Ohmic or Ohmic−Schottky contacts. Of course, the piezoresistance effect also made a contribution to tune the contact, but it would not change the overall $I-V$ symmetry of the device.

Both piezoelectric effect and photoexcitation intensity can tune the $I-V$ transport property of a ZnO microwire device, but they act in opposite directions. By shining the laser at contact A of a device, as the relative intensity of the light being changed *via* optical filters from transmission coefficient $T = 0.001$ to $T = 1$, the $I-V$ curve has been largely tuned (Figure 5a). Fine-tuning of the magnitude of mechanical straining and the intensity of the light illumination can produce a designed shape of the $I-V$ characteristic. Figure 5b shows the coupled tuning of the two effects on the $I-V$ shape. By choosing a strain of −0.2% and relative light intensity $T = 0.01$ (green curve), the observed $I-V$ curve matched well to the original $I-V$ curve obtained without applying a strain and laser excitation (dark curve).

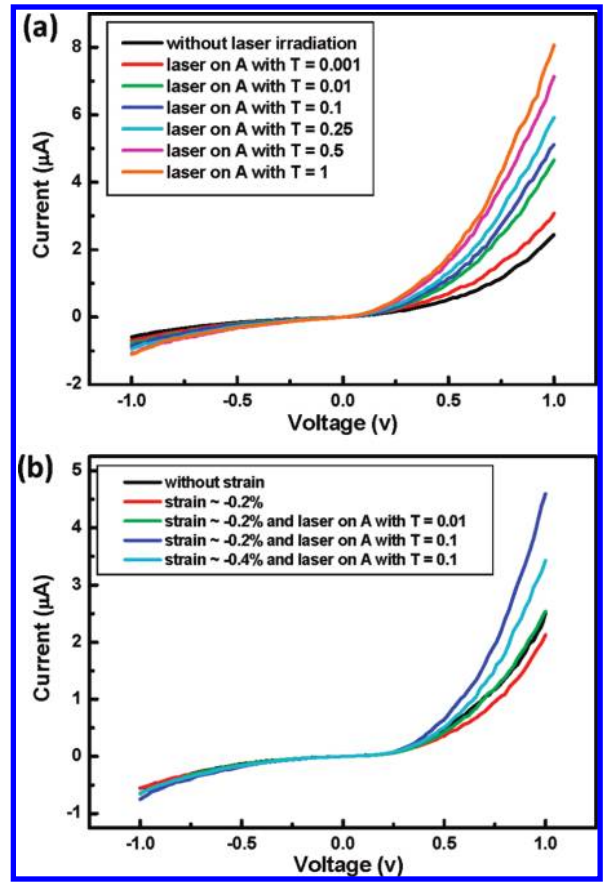

Figure 5. (a) Tuning the $I-V$ transport characteristic of a device by controlling the intensity of the excitation laser focused at contact A *via* optical filters from transmission coefficient $T = 0.001$ to $T = 1$, without strain. (b) Design and control of the transport properties of the device by coupling the intensity of illuminating laser and the degree of straining in the microwire showing the basic principle of piezo-phototronics.

CONCLUSION

In summary, piezoelectricity and photoresponse are two prominent properties of ZnO. We have investigated the localized coupling effect between piezoelectric and photoexcitation properties of ZnO micro/nanowires on the electric transport characteristics of micro/nanowire devices. The piezoelectric effect tends to raise the height of the local Schottky barrier (SB) at a metal−ZnO contact, while the photoexcitation using a light that has energy larger than the band gap of ZnO lowers the SB height. Both effects have equivalent results but in opposite directions. By tuning the relative contributions of the effects from piezoelectricity *via* strain and photoexcitation *via* light intensity, the local contact can be tuned step-by-step and/or transformed from Schottky to Ohmic or from Ohmic to Schottky. After studying the devices with Schottky−Ohmic, Ohmic−Ohmic, and Schottky−Schottky contacts, we have found a new principle for controlling and designing the electronic transport property of the device through a coupling among mechanical, photonic, and electrical properties of ZnO nanowires. This can be the basis for fabricating piezo-photoelectronic nanodevices, which are referred to as piezo-phototronic devices.

EXPERIMENTAL METHODS

Ultralong ZnO microwires used in our study were grown by a high-temperature thermal evaporation process.[21] The typical diameter was around 2−6 μm, and the length was several hundred micrometers to several millimeters. Such long microwires were chosen for easy manipulation using a mechanical deformation stage and with consideration of the limited size of the laser spot, but the same principle applies to nanowires. For device fabrication, a ZnO microwire was first laid down on a polystyrene (PS) substrate, and then each end of the wire was fixed to the substrate using silver paste; metal wires were also bonded to a ZnO microwire for electrical measurement. The dimension of the PS substrate was 3.5 mm in length, 5 mm in width and with a thickness of 1 mm. An additional layer of polydimethylsiloxane (PDMS) was used to package the device, and it kept the device mechanically robust under repeated manipulation. The thickness of the PDMS layer was much thinner than the thickness of the PS substrate. A He−Cd laser (with wavelength = 325 nm) was used as the source for photoexcitation. The diameter of the beam was focused to a spot less than ~20 μm. The laser output power was 30 mW. A Keithley 4200 semiconductor characterization system was used to carry out electrical measurements.

Acknowledgment. Research was supported by DARPA (Army/AMCOM/REDSTONE AR, W31P4Q-08-1-0009), BES DOE (DE-FG02-07ER46394), and NSF (DMS0706436, CMMI

0403671). Thanks to Drs. Jun Zhou and Rusen Yang for many technical assistance.

Supporting Information Available: Schematic for understanding the difference in photoelectric responsivity of a Schottky contact at forward and reverse bias; photoelectric response of a device to light sources with excitation energy less than the band gap of ZnO, and the corresponding PL spectrum taken from the device. This material is available free of charge *via* the Internet at http://pubs.acs.org.

REFERENCES AND NOTES

1. Wang, Z. L. ZnO Nanowire and Nanobelt Platform for Nanotechnology. *Mater. Sci. Eng. Rep.* **2009**, *64*, 33–71.
2. Gudiksen, M. S.; Lauhon, L. J.; Wang, J.; Smith, D. C.; Lieber, C. M. Growth of Nanowire Superlattice Structures for Nanoscale Photonics and Electronics. *Nature* **2002**, *415*, 617–620.
3. Wang, Z. L. Towards Self-Powered Nanosystems: From Nanogenerators to Nanopiezotronics. *Adv. Funct. Mater.* **2008**, *18*, 3553–3567.
4. Patolsky, F.; Timko, B. P.; Yu, G.; Fang, Y.; Greytak, A. B.; Zheng, G.; Lieber, C. M. Detection, Stimulation, and Inhibition of Neuronal Signals with High-Density Nanowire Transistor Arrays. *Science* **2006**, *313*, 1100–1104.
5. Yan, R.; Gargas, D.; Yang, P. Nanowire Photonics. *Nat. Photonics* **2009**, *3*, 569–576.
6. Wang, Z. L.; Song, J. H. Piezoelectric Nanogenerators Based on Zinc Oxide Nanowire Arrays. *Science* **2006**, *312*, 242–246.
7. Wang, X. D.; Song, J. H.; Liu, J.; Wang, Z. L. Direct-Current Nanogenerator Driven by Ultrasonic Waves. *Science* **2007**, *316*, 102–105.
8. Qin, Y.; Wang, X. D.; Wang, Z. L. Microfibre Nanowire Hybrid Structure for Energy Scavenging. *Nature* **2008**, *451*, 809–813.
9. Yang, R. S.; Qin, Y.; Li, C.; Zhu, G.; Wang, Z. L. Converting Biomechanical Energy into Electricity by a Muscle-Movement-Driven Nanogenerator. *Nano Lett.* **2009**, *9*, 1201–1205.
10. Wang, X. D.; Zhou, J.; Song, J. H.; Liu, J.; Xu, N. S.; Wang, Z. L. Piezoelectric Field Effect Transistor and Nanoforce Sensor Based on a Single ZnO Nanowire. *Nano Lett.* **2006**, *6*, 2768–2772.
11. He, J. H.; Hsin, C. L.; Liu, J.; Chen, L. J.; Wang, Z. L. Piezoelectric Gated Diode of a Single ZnO Nanowire. *Adv. Mater.* **2007**, *19*, 781–784.
12. Zhou, J.; Gu, Y. D.; Fei, P.; Mai, W. J.; Gao, Y. F.; Yang, R. S.; Bao, G.; Wang, Z. L. Flexible Piezotronic Strain Sensor. *Nano Lett.* **2008**, *8*, 3035–3040.
13. Kind, H.; Yan, H. Q.; Messer, B.; Law, M.; Yang, P. D. Nanowire UV Photodetectors and Optical Switches. *Adv. Mater.* **2002**, *14*, 158–160.
14. Soci, C.; Zhang, A.; Xiang, B.; Dayeh, S. A.; Aplin, D. P. R.; Park, J.; Bao, X. Y.; Lo, Y. H.; Wang, D. ZnO Nanowire UV Photodetectors with High Internal Gain. *Nano Lett.* **2007**, *7*, 1003–1009.
15. Jin, Y. Z.; Wang, J. P.; Sun, B. Q.; Blakesley, J. C.; Greenham, N. C. Solution-Processed Ultraviolet Photodetectors Based on Colloidal ZnO Nanoparticles. *Nano Lett.* **2008**, *8*, 1649–1653.
16. Zhou, J.; Gu, Y. D.; Hu, Y. F.; Mai, W. J.; Yeh, P.-H.; Bao, G.; Sood, A. K.; Polla, D. L.; Wang, Z. L. Gigantic Enhancement in Response and Reset Time of ZnO UV Nanosensor by Utilizing Schottky Contact and Surface Functionalization. *Appl. Phys. Lett.* **2009**, *94*, 191103.
17. Huang, M. H.; Mao, S.; Feick, H.; Yan, H. Q.; Wu, Y. Y.; Kind, H.; Weber, E.; Russo, R.; Yang, P. D. Room-Temperature Ultraviolet Nanowire Nanolasers. *Science* **2001**, *292*, 1897–1899.
18. Pauzaukie, P. J.; Yang, P. D. Nanowire Photonics. *Mater. Today* **2006**, *9*, 36–45.
19. Ryu, Y.; Lee, T. S.; Lubguban, J. A.; White, H. W.; Kim, B. J.; Park, Y. S. Next Generation of Oxide Photonic Devices: ZnO-Based Ultraviolet Light Emitting Diodes. *Appl. Phys. Lett.* **2006**, *88*, 241108.
20. Gao, P.; Wang, Z. Z.; Liu, K. H.; Xu, Z.; Wang, W. L.; Bai, X. D.; Wang, E. G. Photoconducting Response on Bending of Individual ZnO Nanowires. *J. Mater. Chem* **2009**, *19*, 1002–1005.
21. Pan, Z. W.; Dai, Z. R.; Wang, Z. L. Nanobelts of Semiconducting Oxides. *Science* **2001**, *291*, 1947–1949.
22. Sze, S. M. *Physics of Semiconductor Devices*, 2nd ed.; Wiley: New York, 1981.
23. Gao, Z. Y.; Zhou, J.; Gu, Y. D.; Fei, P.; Hao, Y.; Bao, G.; Wang, Z. L. Effects of Piezoelectric Potential on the Transport Characteristics of Metal−ZnO Nanowire−Metal Field Effect Transistor. *J. Appl. Phys. Lett.* **2009**, *105*, 113707.
24. Gao, Y. F.; Wang, Z. L. Equilibrium Potential of Free Charge Carriers in a Bent Piezoelectric Semiconductive Nanowire. *Nano Lett.* **2009**, *9*, 1103–1110.
25. Yeh, P.-H.; Li, Z.; Wang, Z. L. Schottky-Gated Probe-Free ZnO Nanowire Biosensor. *Adv. Mater.* **2009**, *21*, 4975–4978.